

# Imaging of intracellular spherical lamellar structures and tissue gross morphology by a focused ion beam/scanning electron microscope (FIB/SEM)

Damjana Drobne<sup>a,\*</sup>, Marziale Milani<sup>b</sup>, Vladka Lešer<sup>a</sup>, Francesco Tatti<sup>d</sup>, Alexis Zrimec<sup>c</sup>,  
Nada Žnidaršič<sup>a</sup>, Rok Kostanjšek<sup>a</sup>, Jasna Štrus<sup>a</sup>

<sup>a</sup>Department of Biology, University of Ljubljana, Večna pot 111, SI-1000 Ljubljana, Slovenia

<sup>b</sup>Materials Science Department, University of Milano-Bicocca, Via Cozzi 53, I-20125 Milano, Italy

<sup>c</sup>Institute of Physical Biology, Velika Loka 90, SI-1290 Grosuplje, Slovenia

<sup>d</sup>FEI Italia, Via Cervi 40, I-00139 Roma, Italy

Received 16 August 2006; received in revised form 12 October 2007; accepted 26 October 2007

## Abstract

We report the use of a focused ion beam/scanning electron microscope (FIB/SEM) for simultaneous investigation of digestive gland epithelium gross morphology and ultrastructure of multilamellar intracellular structures. Digestive glands of a terrestrial isopod (*Porcellio scaber*, Isopoda, Crustacea) were examined by FIB/SEM and by transmission electron microscopy (TEM). The results obtained by FIB/SEM and by TEM are comparable and complementary. The FIB/SEM shows the same ultrastructural complexity of multilamellar intracellular structures as indicated by TEM. The term lamellar bodies was used for the multilamellar structures in the digestive glands of *P. scaber* due to their structural similarity to the lamellar bodies found in vertebrate lungs. Lamellar bodies in digestive glands of different animals vary in their abundance, and number as well as the thickness of concentric lamellae per lamellar body. FIB/SEM revealed a connection between digestive gland gross morphological features and the structure of lamellar bodies. Serial slicing and imaging of cells enables easy identification of the contact between a lamellar body and a lipid droplet. There are frequent reports of multilamellar intracellular structures in different vertebrate as well as invertebrate cells, but laminated cellular structures are still poorly known. The FIB/SEM can significantly contribute to the structural knowledge and is always recommended when a link between gross morphology and ultrastructure is investigated, especially when cells or cellular inclusions have a dynamic nature due to normal, stressed or pathological conditions.

© 2007 Published by Elsevier B.V.

PACS: 87.14.Cc; 87.16.-b; 87.16.Dg; 87.64.Ee

Keywords: Focused ion beam; Scanning electron microscopy; Crustacea; Isopoda; Hepatopancreas

## 1. Introduction

Currently there are numerous microscopy methods available to provide subcellular structural information at resolutions as low as 1–2 nm [1–3] but simultaneous imaging of intracellular structures and tissue gross

morphology continues to be a challenge in the structural investigation of biological samples. Recently, focused ion beam/scanning electron microscopes (FIB/SEM) have been used in the field of life sciences [4–11] and offer an attractive possibility with which to expand sample surface investigations by subsurface structural research at any location of interest. The introduction of FIB for *in situ* exposure of subsurface structures has the potential to produce structural information on biological samples that may be overlooked or missed when switching from

\*Corresponding author. Tel.: +386 1 4233388; fax: +386 1 2573390.

E-mail address: [damjana.drobne@bf.uni-lj.si](mailto:damjana.drobne@bf.uni-lj.si) (D. Drobne).

surface investigation performed by conventional SEM to transmission electron microscopy (TEM) ultrastructural research.

The FIB/SEM system is a combination of a focused ion beam, an electron beam and secondary ion and/or secondary electron detectors. A focused ion beam of gallium ( $\text{Ga}^+$ ) ions at low beam currents is used for imaging, and high beam currents are used for site specific *in situ* sputtering or milling. The signals from the sputtered secondary ions or secondary electrons are collected to form an image [12]. FIB/SEM investigation is applied to bulk samples prepared for conventional scanning electron microscopy or on bulk resin-embedded specimens at any chosen site [11]. The imaging resolution of the FIB/SEM system theoretically achievable on biological samples, where the field emission gun (FEG SEM) is used at a low accelerating voltage of  $5 \leq \text{keV}$ , is 1 nm [11,13].

In this study, we tested the applicability of a FIB/SEM system for simultaneous ultrastructural research into multilamellar intracellular structures and morphological characteristics of the tissue. Multilamellar cellular structures are frequently present in various vertebrate and invertebrate cell types under normal, stressed and pathological conditions. The concentric or stack-like intracellular lamellar structures have a variety of names. In the older literature, laminated membranous structures were mainly termed myelinoid bodies or myelinosomes. More recently, those that serve as specialized lipid storage and secretory organelles in some vertebrate cell types and which have multilamellar structures from 100 to 2400 nm in diameter, are termed lamellar bodies. They are lysosome-related organelles [14–21]. The best known and most investigated

lamellar bodies are produced by pneumocyte II cells [18,19,21–26].

The structural appearance and abundance of intracellular lamellar inclusions in vertebrate cells change in many diseases and stressed conditions and as a result of action of agents with different pharmacological profiles [15,17,27–35].

In invertebrates, multilamellar intracellular structures have also been frequently found in a variety of tissues and organisms and have been given different names. In insects, they were described in fat bodies [36], in midgut [37,38], and in pheromone-secreting mandibular glands [39]. They were found also in the cell nucleus of young oocytes after

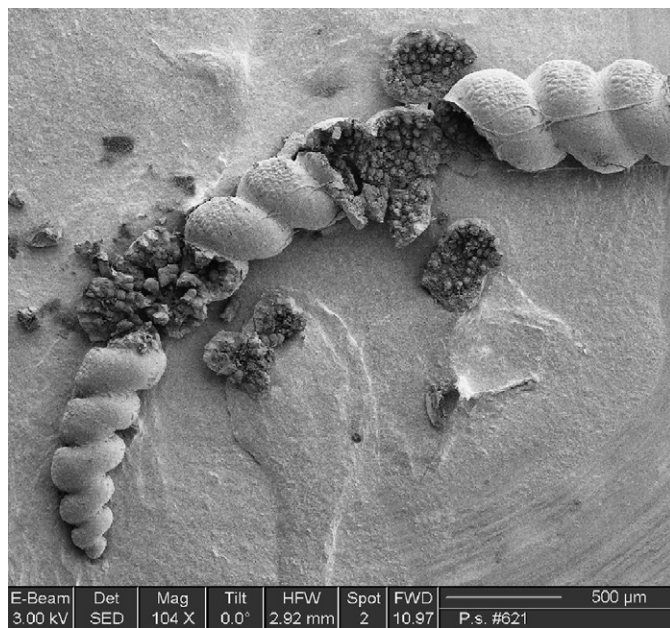


Fig. 1. A manually opened digestive gland tube: scanning electron micrograph of posterior two-thirds of partly opened gland tube.

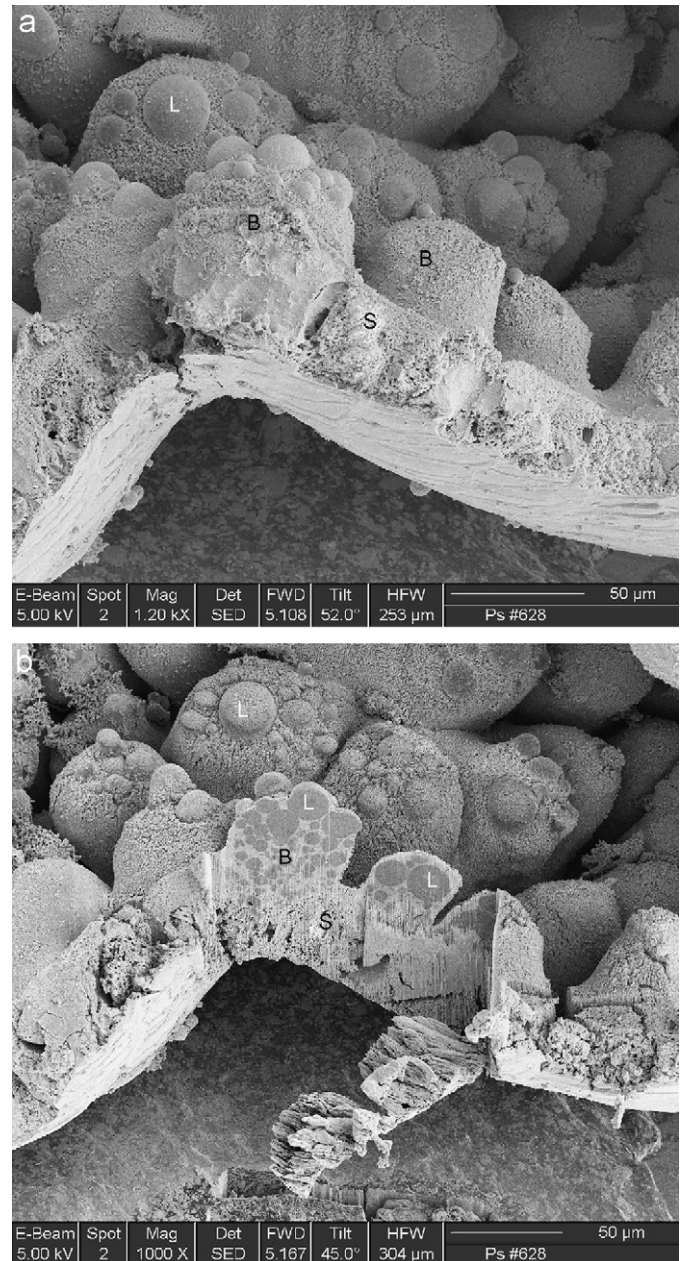


Fig. 2. An FIB milled digestive gland epithelium: scanning electron micrographs of large B- and small S-cells of hepatopancreas before (a) and after (b) FIB milling. L—lipid droplet, S—S-cell, B—B-cell.

exposure of the earthworm to cadmium [40]. Multilamellar intracellular structures have often been detected in the digestive system of different crustacean species [41–46]. In isopod crustaceans, they were found in normal hepatopancreatic cells, but at increased levels in metal-stressed animals [45].

The most detailed morphological description of multilamellar cellular structures has been provided for lamellar bodies in lung tissue [20,47–49]. Lamellar bodies were described as membrane-bound granules composed of densely packed monolayer lamellae, with a unit membrane-like structure and thickness. Some lamellae were reported to have intramembranous particles and others were described as having a smooth surface [48]. Freeze–fracture replica techniques enabled the estimation of the thickness of lamellae which was approximately 10 nm [48]. In some lamellar bodies, lamellae are concentrically oriented and in others, a single lamella reverses its direction to form a closed sac and the strip-like appearance of a lamellar body [48].

In our work, a FIB/FEG SEM system was employed for simultaneous investigation of the digestive gland epithelium gross morphology and the ultrastructure of multilamellar intracellular structures in isopod crustacean (*Porcellio scaber*, Isopoda, Crustacea). Isopod digestive glands (hepatopancreas) have been intensively investigated

by means of light microscopy, and scanning and TEM [7–9,44–46,50,51]. Multilamellar intracellular structures were detected in the digestive glands under normal and stressed conditions, but their morphology has not been described in detail [44–46].

In the work presented here:

- the FIB/SEM system was used for simultaneous structural study of multilamellar cellular structures in hepatopancreas of *P. scaber* and the gross morphology of the digestive gland epithelium;
- the structural characteristics of multilamellar intracellular structures obtained by FIB/SEM and TEM were compared;
- successive FIB sectioning and SEM imaging were performed to reveal the contact between a multilamellar inclusion and a lipid body.

The perspectives of FIB/SEM for structural research of biological samples are discussed.

## 2. Material and methods

Terrestrial isopods, *P. scaber* (Latreille, 1809) (Isopoda, Crustacea), were collected from under concrete blocks and pieces of decaying wood.

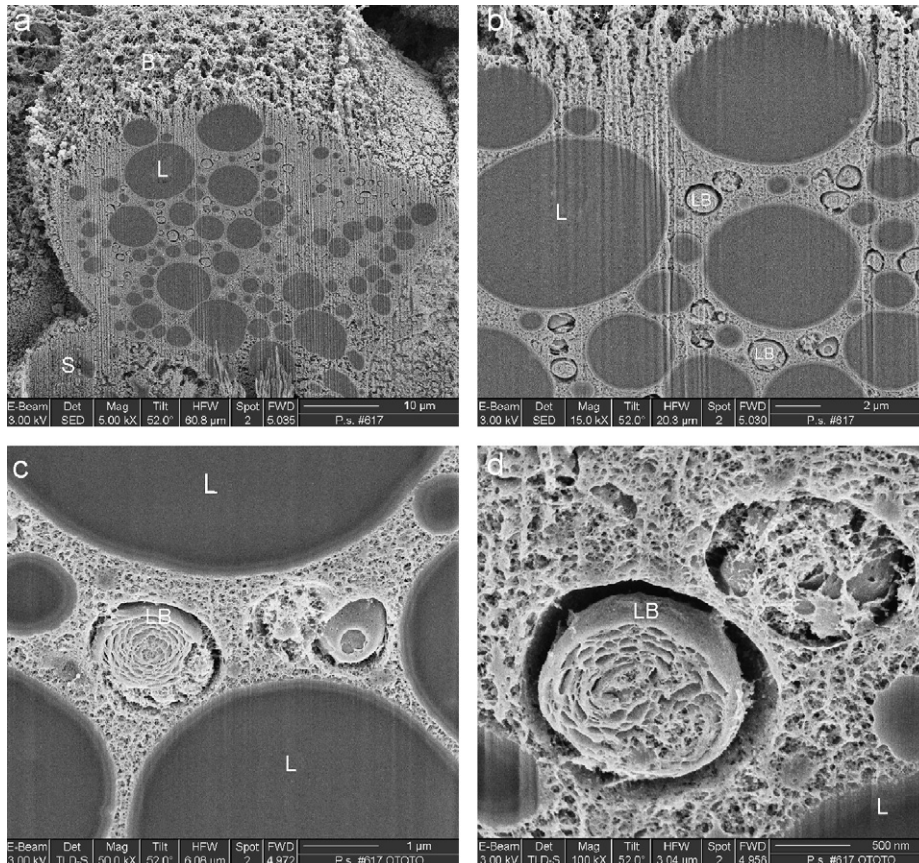


Fig. 3. An FIB milled B-cell, which is in the extruding phase: scanning electron micrographs of FIB exposed interior of a B-cell. Asterisk—disintegrated apical part of a cell, L—lipid droplet, LB—lamellar body.

### 2.1. Sample preparation for FIB/SEM

Digestive gland tubes (hepatopancreas) were fixed in 1.0% glutaraldehyde and 0.4% paraformaldehyde in 0.1 M sodium cacodylate buffer (pH 7.2) for 2.5 h at room temperature. The chemically fixed samples were processed by OTOTO (OsO<sub>4</sub>/thiocarbohydrazide/OsO<sub>4</sub>/thiocarbohydrazide/OsO<sub>4</sub>) [52]. After dehydration in a graded series of ethanol solutions, the samples were dried at the critical point (Balzers Critical Point Dryer 030) and gold sputtered (Sputter coater SCD 050, BAL-TEC, Germany). Digestive glands of a total of eight animals were investigated by the FIB/SEM system.

### 2.2. FIB/SEM operation

The samples were fixed on brass holders with high purity silver paint (SPI) and mounted on carbon discs fixed on aluminium holders. Samples were stored in a dessicator until analysis. In the chamber of the FIB/SEM system (FEI Strata DB 235M dual beam, Modena University, Italy) the samples (usually four at once) were fixed on a silicon wafer holder (5 cm diameter, 6-axis eucentric stage). The ion currents for milling were between of 5 and 7 nA, the beam energy was approximately 30 keV Ga<sup>+</sup>. Lower beam currents were used for the cleaning mill

and were in the range of 0.3–1 nA. Ions were field-emitted from a liquid metal ion source. The spot size in the case of milling was approximately 200–300 nm in diameter, and in cleaning approximately 50–100 nm in diameter. The dwell time for milling was 1 μs/spot and the overlap was 50%. SEM imaging was performed by the field emission (FE) electron column available in the same system. The spot size in the case of SEM varied up to 5 nm in diameter. In FIB/SEM, secondary electron detectors were used to collect the signal produced by a primary electron beam.

FIB milling and SEM imaging were performed in 2–4 cells in the median parts of the gland tubes. One or two of a total of four tubes were investigated in each animal.

### 2.3. Sample preparation for TEM

The tissue for TEM was fixed in 3.5% glutaraldehyde in 0.1 M phosphate buffer (3–4 h), rinsed in the same buffer, postfixed in 1% OsO<sub>4</sub> (1 h), dehydrated in ethanol and embedded in Spurr's resin. Ultrathin sections (Reichert Ultracut S) were stained with uranyl acetate and lead citrate. Samples were inspected with a CM 100 Philips microscope and images documented with BioScan 792 camera (Gatan).

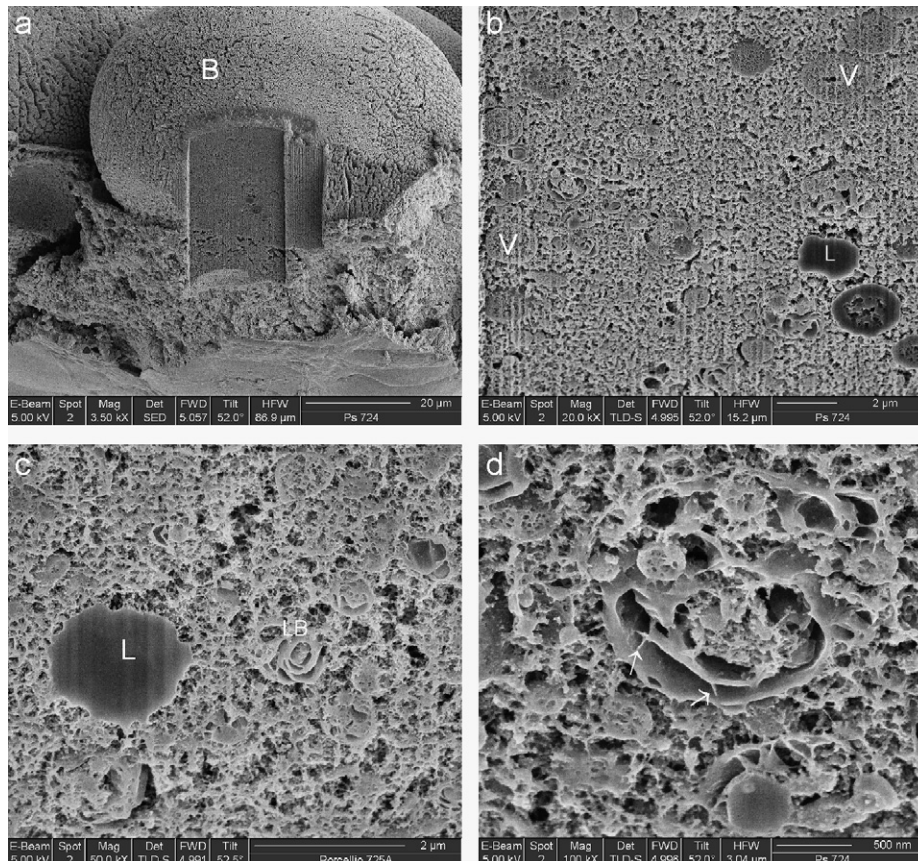


Fig. 4. An FIB milled B-cell, which is in the non-extruding phase of the digestive cycle: scanning electron micrographs of FIB exposed interior of a B-cell. L—lipid droplet, LB—lamellar body, V—vesicles with net-like material, arrows—lamellar connections between the two adjacent lamellae.

### 3. Results

Digestive glands (hepatopancreas) of *P. scaber* are composed of four spiral blind-ended tubes. Two-thirds (the posterior and middle parts) of a manually opened tube are shown in Fig. 1. The hepatopancreatic epithelium consists of two cell types, large B- and small S-cells wedged in between B-cells (Figs. 2a and b). We investigated the ultrastructure of B-cells in the medioposterior part of gland tubes of eight animals. In some of the gland tubes investigated, B-cells were filled with lipid droplets (Figs. 2a, b and 3a–d) and some of these extruded their content into the gland lumen (Figs. 2a and b). In other animals, B-cells contained fewer lipid droplets and extrusion of cellular content into the gland lumen was not detected (Fig. 4a).

The FIB milling of gland epithelium exposed the interior of B- and S-cells (Figs. 2a and b, 3a–d, 4a–d and 6a–f). The most prominent ultrastructural elements of B-cells were lipid droplets of different sizes, and spherical multilamellar intracellular structures. Due to structural similarities of multilamellar structures found in the hepatopancreatic cells with lamellar bodies reported previously, we use this term. The diameter of lamellar bodies is in general 0.5  $\mu\text{m}$ , but sometimes it can be as much as 1  $\mu\text{m}$  (Figs. 3a–d, 4d, 6a–f). The core of a multilamellar structure was observed in some cases to be composed of dense material (Fig. 6c).

Lamellar bodies were detected in all the animals investigated. There were no differences in the appearance of lamellar bodies when different cells of the same tube or of different tubes of the same animal were compared (Figs. 3a–d and 6a–f). However, the abundance of lamellar bodies, the thickness of concentric lamellae in a lamellar body and number of lamellae in the lamellar body varied among the animals. In three of the eight animals investigated by FIB/SEM, the concentric lamellae were thin and there were more than five concentric lamellae in the lamellar body (Figs. 3c, d and 6a–f). In five of the eight animals investigated, the concentric lamellae were thick (Figs. 4c and d). There were less than five concentric lamellae in the lamellar body.

On the basis of conventional TEM analysis of the B-cells' ultrastructure, multilamellar concentric spherical structures described by FIB/SEM would appear to correspond to the multilayered vesicles displayed on TEM images (Figs. 5a, b and 7). Our suggestion, that the FIB/SEM and TEM images represent the same type of structure in B-cells, is based on the following ultrastructural criteria: spherical shape; a diameter around 1  $\mu\text{m}$ ; concentrically arranged lamellae; frequent grouping of these structures and association with lipid droplets.

Occasionally, lamellar bodies were observed to be associated with lipid droplets (Figs. 6a–f and 7). Subsequent serial FIB milling operations revealed the core of the lipid body surrounded by a thick envelope and in close association with the lamellae of a multilamellar structure.

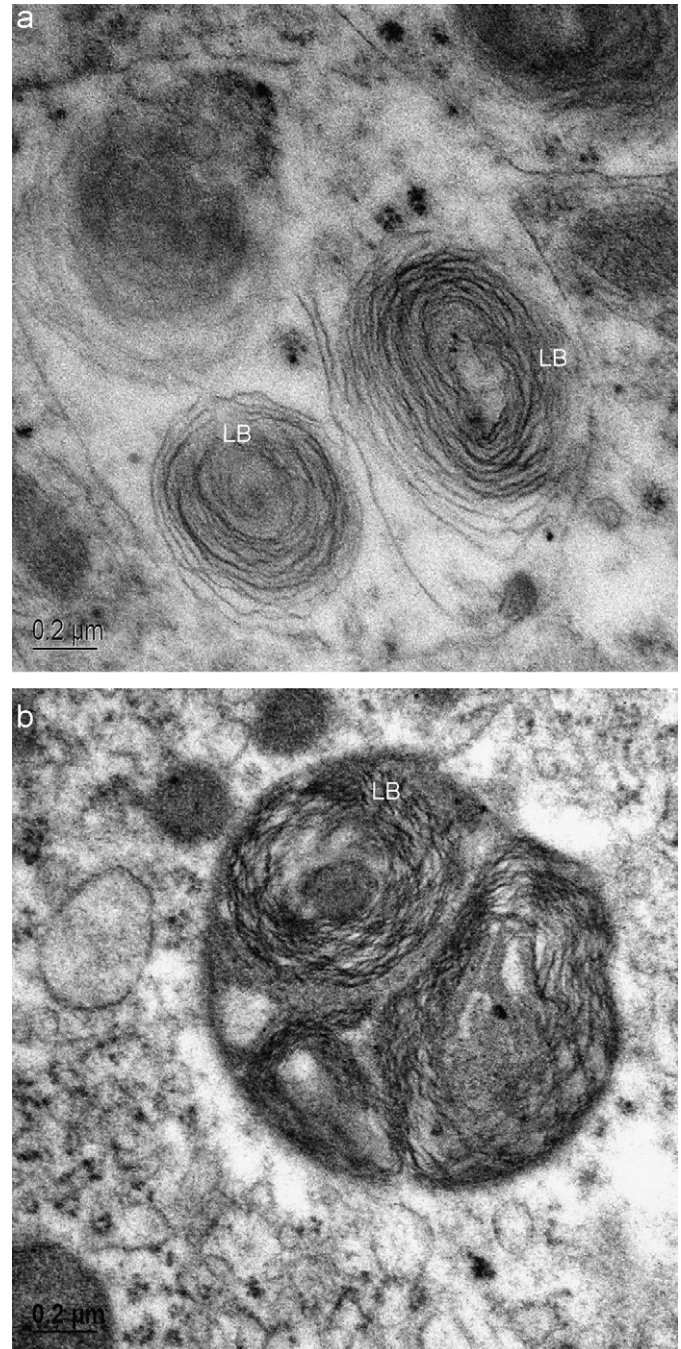


Fig. 5. Lamellar bodies imaged by TEM: transmission electron micrograph of lamellar bodies in two different animals.

Lamellar bodies were also observed to contain net-like and/or granular material (Figs. 3b–d, 4d, 5a, and b).

The ultrastructural variability of lamellar bodies in isopod hepatopancreatic cells is manifested in different numbers and thickness of concentric lamellae and in the variety of associations with other cellular structures. The highest ultrastructural variability of lamellar bodies was observed in non-extruding hepatopancreatic cells (Figs. 4a–d). In the extruding cells, the number of concentric lamellae per lamellar body was always higher

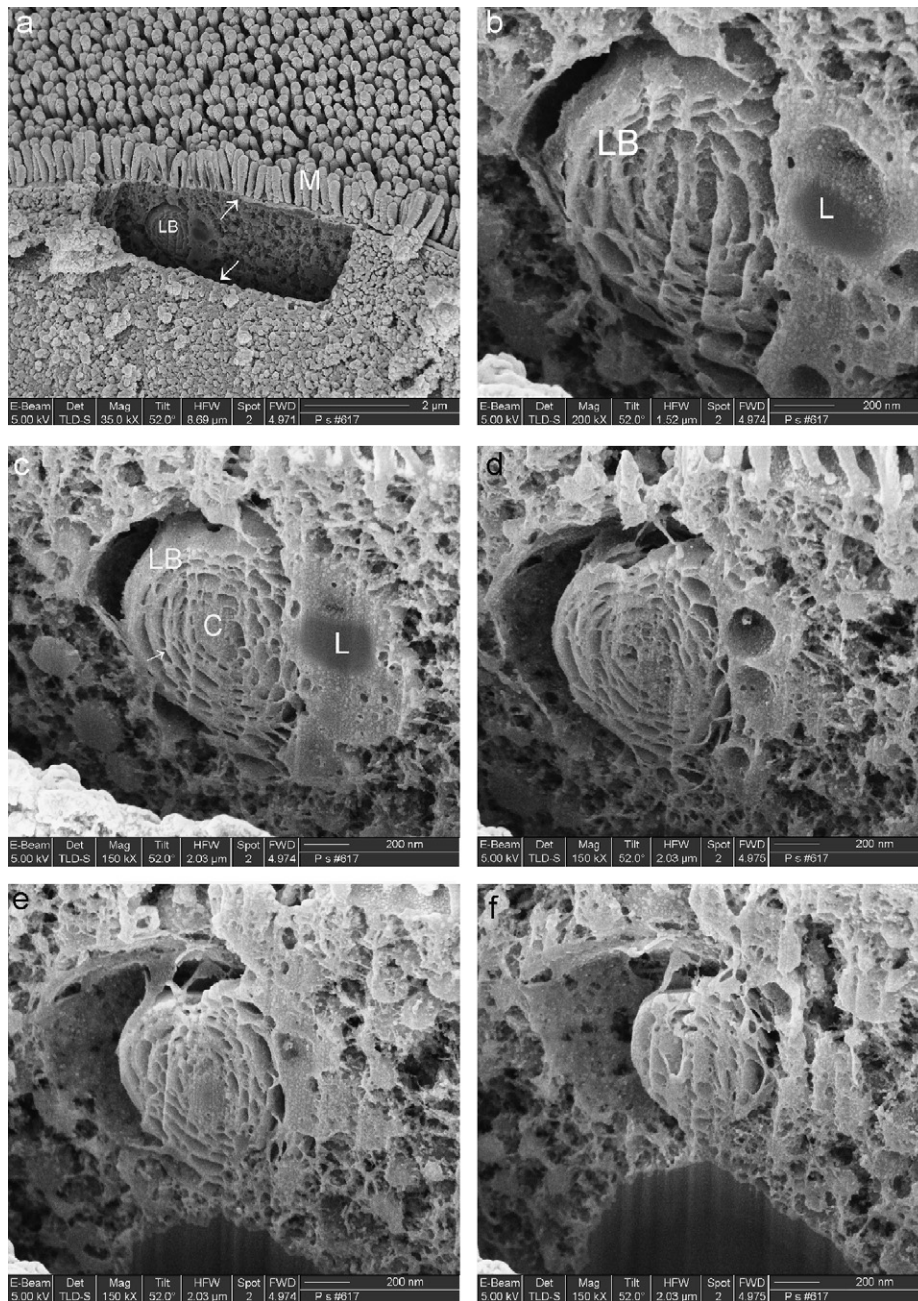


Fig. 6. Successive milling of a lamellar body and lipid droplet: scanning electron micrographs of six successive milling operations that gradually reveal the association between a multilamellar body and a lipid droplet. M—microvilli, L—lipid droplet, LB—lamellar body, C—core of a lamellar body, arrows—edges of milled trench (a), arrow—lamellar connections between the two adjacent lamellae (c).

than those in the non-extruding cells and they had a more regular concentric arrangement (Figs. 3a–d).

Successive milling operations were performed to reveal the association between a lamellar body and a lipid droplet (Figs. 6a–d). After repeated milling, the ultrastructure of the milled lamellar body remained unaffected (Figs. 6a–d).

Ultrastructural information on lamellar bodies obtained by FIB/SEM is in accordance with that revealed by conventional TEM (Figs. 3a–d, 5a, b, 6a–f and 7). The advantage of the FIB/SEM system is that it enables

topographical imaging of any selected lamellar body and at the same time provides information on the gross morphology of the investigated organ/tissue (hepatopancreas).

#### 4. Discussion

We have demonstrated that FIB/SEM is suitable for simultaneous investigation of sample surfaces and subsurface structures. In SEM the contrast is based primarily on specimen topography and in TEM on the number of

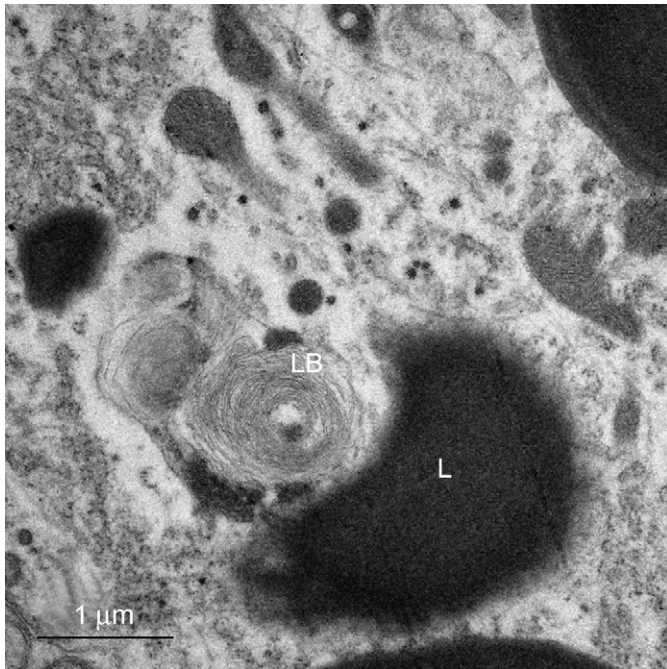


Fig. 7. Lamellar body in a close association with a lipid body imaged by TEM: transmission electron micrograph of a lamellar body attached to a lipid body.

electrons transmitted through the specimen, and consequently, the cell ultrastructures imaged by SEM or TEM appeared different. However, multilamellar intracellular structures and lipid bodies in digestive glands of a terrestrial isopod *P. scaber* show the same characteristics when examined by FIB/SEM or by TEM.

The ultrastructure of multilamellar intracellular inclusions in the digestive glands of *P. scaber*, resembles that of lamellar bodies described in the literature, and we employ this term. Lamellar bodies were found in B-cells of hepatopancreas in all investigated animals. Their number, size and ultrastructure vary, but most commonly, they have concentric periodicity of the lamellae. The same ultrastructural appearance of lamellar bodies was observed by TEM in vertebrate type II pneumocytes [18–20, 22–24, 27, 53–55], in posterior midgut gland ceca of the decapod crustacean, *Lepidophthalmus lousianensis* (Decapoda, Crustacea) [42] and in hepatopancreas of the terrestrial isopod *P. scaber* (Isopoda, Crustacea) [44–46]. Our results confirm the dynamic nature and the structure of the lamellar bodies in the hepatopancreatic cells.

We observed a connection between digestive gland gross morphological characteristics (extruding and non-extruding phase of a cell) and the structure of lamellar bodies. How the structural variability of lamellar bodies is related to the function of hepatopancreatic cells remains to be investigated and FIB/SEM appears to be a very suitable tool for such type of structural research.

We found close and various kinds of associations of lamellar bodies and lipid bodies which are in agreement with published data and consistent with their function

[21,33]. The major known role of lamellar bodies is in the supply and turnover of certain lipids between organs within the organism. The role of lamellar bodies in the isopod hepatopancreatic cells however is not clear.

The FIB/SEM investigation of biological cells and tissue has been conducted by other laboratories [11,56–58]. The FIB/SEM was used preferably on embedded biological samples. On the basis of the results presented in this study, we encourage the use of the FIB/SEM on biological samples prepared for conventional SEM. The aim of such an approach is to establish a link between larger scale tissue morphology and cellular and subcellular structures. We believe that the ability to reveal specific intracellular structural details and to link them to the gross morphology of the tissue or organ is currently among most promising and beneficial applications of FIB/SEM in life sciences. This is of particular interest when cells or cellular inclusions have a dynamic nature due to normal, stressed or pathologic conditions.

## 5. Conclusions

1. The FIB/SEM has demonstrated the same ultrastructural complexity of lamellar bodies as indicated by TEM.
2. As revealed by TEM, close and various kinds of associations of lamellar bodies and lipid bodies were found.
3. Since the SEM and TEM differ in image formation, the images obtained by the two methods are complementary but not redundant.
4. FIB/SEM reveals a connection between the gross morphological features of the digestive gland and the structure of lamellar bodies. Such a connection could not be easily demonstrated by conventional electron microscopy.
5. We successfully generated 50 nm successive FIB sections of chemically fixed and critical point dried samples and we easily identified the contact between a lamellar body and a lipid droplet.

## Acknowledgements

The cooperation among authors of this work was supported by the Italian Ministry for Foreign Affairs and the Slovenian Ministry of Higher Education, Science and Technology (Grant SLO-ITA VŽ3/2005–2008), and the Slovenian Research Agency, through Grant # J1-3186.

## References

- [1] R. McIntosh, D. Nicastro, D. Mastrorade, Trends Cell. Biol. 15 (2005) 43.
- [2] W. Baumeister, Protein Sci 14 (2005) 257.
- [3] O. Medalia, I. Weber, A.S. Frangakis, D. Nicastro, G. Gerisch, W. Baumeister, Science 298 (2002) 1209.
- [4] J. Li, JOM 58 (2006) 27.

- [5] M. Milani, M. Ballerini, D. Batani, F. Squadrini, F. Cotelli, C.L.L. Donin, G. Poletti, A. Pozzi, K. Eidmann, A. Stead, G. Lucchini, *Eur. Phys. J. Appl. Phys.* 26 (2004) 123.
- [6] M. Milani, D. Drobne, F. Tatti, D. Batani, G. Poletti, F. Orsini, A. Zullini, A. Zrimec, *Scanning* 27 (2005) 249.
- [7] D. Drobne, M. Milani, M. Ballerini, A. Zrimec, M. Berden Zrimec, F. Tatti, K. Drašlar, *J. Biomed. Opt.* 9 (2004) 1238.
- [8] D. Drobne, M. Milani, A. Zrimec, M. Berden Zrimec, F. Tatti, *K. Drašlar, Scanning* 27 (2005) 30.
- [9] D. Drobne, M. Milani, A. Zrimec, V. Lešer, M. Berden Zrimec, *J. Microsc. (Oxford)* 210 (2005) 29.
- [10] M. Milani, D. Drobne, *Scanning* 28 (2006) 148.
- [11] J.A.W. Heymann, M. Hayles, I. Gestmann, L.A. Giannuzzi, B. Lich, S. Subramaniam, *J. Struct. Biol.* 155 (2006) 63.
- [12] P.J. Goodhew, J. Humphreys, R. Beanland, *Electron Microscopy and Analyses*, Tylor & Francis, London, 2001.
- [13] S.L. Erlandsen, C. Frethem, Y. Chen, *J. Histotechnol.* 23 (2000) 249.
- [14] Y. Satoh, A.P. Gesase, Y. Habara, K. Ono, T. Kanno, *Microsc. Res. Tech.* 34 (1996) 104.
- [15] F.N. Ghadially, *Ultrastructural Pathology of Cell and Matrix*, Butterworth–Heinemann, Boston, 1997.
- [16] G. Vogt, H. Segner, *Cell Tissue Res.* 289 (1997) 191.
- [17] G. Schmitz, G. Mueller, *J. Lipid Res.* 32 (1991) 1539.
- [18] T.E. Weaver, C.L. Na, M. Stahlman, *Cell Dev. Biol.* 13 (2002) 263.
- [19] M.T. Stahlman, M.P. Gray, M.W. Falconieri, J.A. Whitsett, T.E. Weaver, *Lab. Invest.* 80 (2000) 395.
- [20] K.N. Michailova, *Anat. Embryol.* 208 (2004) 301.
- [21] R. Ridsdale, M. Post, *Am. J. Physiol. Lung Cell Mol. Physiol.* 287 (2004) L743.
- [22] J. Gil, O.K. Reiss, *J. Cell Biol.* 58 (1973) 152.
- [23] Jain, J. Martensson, T. Mehta, A.N. Krauss, P.A.M. Auld, A. Meister, *Proc. Natl. Acad. Sci. USA* 89 (1992) 5093.
- [24] M.R. Chinoy, L.W. Gonzales, P.L. Ballard, A.B. Fisher, R.G. Eckenhoff, *Am. J. Resir. Cell Mol. Biol.* 13 (1995) 99.
- [25] J.C. Condon, F. Jeyasuria, J.M. Faust, C.R. Mendelson, *Proc. Natl. Acad. Sci. USA* 101 (2004) 4978.
- [26] Benachi, J.M. Jouannic, A.M. Barlier-Mur, B. Chailley-Heu, J.R. Bourbon, *Am. J. Physiol.—Lung C* 288 (2005) L562.
- [27] Botas, F. Poulain, J. Akiyama, C. Brown, L. Allen, J. Goerke, J. Clements, E. Carlson, A.M. Gillespie, C. Epstein, S. Hawgood, *Proc. Natl. Acad. Sci. USA* 95 (1998) 11869.
- [28] E. Cutz, S.E. Wert, L.M. Noguee, A.M. Moore, *Am. J. Respir. Crit. Care Med.* 161 (2000) 608.
- [29] K. Williams, D. Malarkey, L. Cohn, D. Patrick, J. Dye, G. Toews, *Chest* 125 (2004) 2278.
- [30] V. Edwards, E. Cutz, S. Viero, A.M. Moore, L. Noguee, *Ultrastruct. Pathol.* 29 (2005) 503.
- [31] X.Y. Tang, S. Yamanaka, Y. Miyagi, Y. Nagashima, Y. Nakatani, *Pathol. Int.* 55 (2005) 137.
- [32] Köhler, E. Wahl, K. Soffker, *Environ. Toxicol. Chem.* 21 (2002) 2434.
- [33] P. Lajoie, G. Guay, J.W. Dennis, I.R. Nabi, *J. Cell Sci.* 118 (2005) 1991.
- [34] G. Kroemer, M. Jäättelä, *Nat. Rev. Cancer* 5 (2005) 886.
- [35] W. Martinet, G.R.Y. De Meyer, L. Andries, A.G. Herman, M.M. Kockx, *J. Histochem. Cytochem.* 54 (2006) 85.
- [36] M. Locke, *Ann. Rev. Entomol.* 48 (2003) 1.
- [37] W. Nopanitaya, D.W. Misch, *Tissue Cell* 6 (1974) 487.
- [38] M. Pawert, R. Triebkorn, S. Graff, M. Berkus, J. Schulz, H.R. Köhler, *Sci. Total Environ.* 181 (1996) 187.
- [39] L.F. Gracioli, R.L.M.S. de Moraes, C. Cruz-Landim, *Micron* 35 (2004) 331.
- [40] E. Siekierska, D. Urbanska-Jasik, *Environ. Pollut.* 120 (2002) 289.
- [41] T.W. Schultz, *J. Morphol.* 149 (1976) 383.
- [42] D.L. Felder, B.E. Felgenhauer, *Acta Zool.* 74 (1993) 263.
- [43] L. Herrera-Alvarez, I. Fernandez, J. Benito, F. Pardos F, J. Morphol. 244 (2000) 177.
- [44] V. Storch, *Symp. Zool. Soc. Lond.* 53 (1984) 167.
- [45] H.R. Köhler, K. Huttenrauch, M. Berkus, S. Graff, G. Alberti, *Appl. Soil Ecol.* 3 (1996) 1.
- [46] N. Žnidaršič, J. Štrus, D. Drobne, *Environ. Toxicol. Pharmacol.* 13 (2003) 161.
- [47] C.J. Stratton, *Cell Tissue Res.* 193 (1978) 219.
- [48] M.C. Williams, *Exp. Lung Res.* 4 (1982) 37.
- [49] S. Shimura, T. Aoki, T. Takishima, *Respiration* 50 (1986) 139.
- [50] C.A.C. Hames, S.P. Hopkin, *Can. J. Zool.* 69 (1991) 1931.
- [51] D. Drobne, J. Štrus, *Environ. Toxicol. Chem.* 15 (1996) 126.
- [52] E.A. Dunnebie, J.M. Segenhout, D. Kalicharan, W.L. Jongebloed, H.P. Wit, F.W.J. Albers, *J. Speech. Lang. Hear. Res.* 90 (1995) 139.
- [53] M. Ochs, H. Fehrenbach, J. Richter, *Anatom. Record* 277A (2004) 287.
- [54] M. Hariri, G. Millane, M.P. Guimond, G. Guay, J.W. Dennis, I.R. Nabi, *Mol. Biol. Cell* 11 (2000) 255.
- [55] M. Ochs, H. Fehrenbach, J. Richter, *Anat. Rec.* 263 (2001) 118.
- [56] T. Kamino, T. Yaguchi, T. Ohnishi, T. Ishitani, M. Osumi, *J. Electr. Microsc.* 53 (2004) 563.
- [57] T. Iwanami, Y. Liu, M. Okazaki, M. Nojima, T. Sakamoto, M. Owari, *Surf. Interf. Anal.* 38 (2006) 1658.
- [58] M. Marko, C. Hsieh, R. Schalek, J. Frank, C. Mannella, *Nature Methods* 4 (2007) 215.